Birkeland, K.W., K. Kronholm, S. Logan, and J. Schweizer (2006), Field measurements after fracture of snowpack weak layers, Geophysical Research Letters, 33, L03501, doi:10.1029/2005GL025104.

To view the published open abstract, go to http://dx.doi.org and enter the DOI.

Field measurements of sintering after fracture of snowpack weak layers

Karl W. Birkeland[1,2], Kalle Kronholm[2,3,5], Spencer Logan[2,4] and Jürg Schweizer[5,*]

[1]USDA Forest Service National Avalanche Center, Box 130, Bozeman, MT 59771, USA
[2]Department of Earth Sciences, Montana State University, Bozeman, MT 59717, USA
[3] Now at Norwegian Geotechnical Institute, Box 3930 Ullevål Stadion, N-0806 Oslo, Norway
[4] Now at Colorado Avalanche Information Center, 325 Broadway, WS1, Boulder, CO 80305, USA
[5]WSL Swiss Federal Institute for Snow and Avalanche Research SLF, Flüelastrasse 11, CH-7260 Davos Dorf, Switzerland

Abstract

This research documents two cases where field workers unintentionally fractured a snowpack weak layer, but no avalanche released. Measurements from before and after the fractures provide unique data sets on the temporal change of snow stability. Shear strength decreased immediately after fracture on both slopes. Subsequent strengthening occurred in both cases, though the rates differed presumably due to the characteristics of the weak layers. Our results have two important implications. First, they suggest the sub-critical weak layer fractures assumed as a prerequisite in some snow slab avalanche release models are transient features, and future modeling efforts must take this into account. Second, they provide insights into interpreting snow stability tests and assessing the stability of slopes with fractured weak layers.
INDEX TERMS: 0736 Snow; 0742 Avalanches

* Corresponding author: schweizer@slf.ch

1. Introduction

The complex, layered structure of the seasonal snowpack is a prerequisite for slab avalanche formation [*Colbeck*, 1991]. Dry slab avalanches occur on steep slopes when a weak layer or a weak interface below a cohesive slab layer fractures [*Schweizer, et al.*, 2003]. Most snow slab release models assume a slope parallel failure (in mode II and III) beneath the slab driven by stress concentrations that form at the boundary of the fractured area [*McClung,* 1979; 1981]. When the crack reaches a critical size, estimated to be on the order of 0.1 to 10 m [*Schweizer*, 1999], the energy released due to a slight expansion of the crack exceeds the energy dissipation related to crack opening, resulting in conditions for fast, catastrophic fracture propagation [*Louchet,* 2001]. Finally, the peripheral support of the slab is overcome, releasing a slab avalanche.

Many numerical models of natural snow slab avalanche release [e.g., *Bader and Salm,* 1990; *Stoffel and Bartelt*, 2003] assume a shear crack propagation criterion based on the classical fracture mechanical energy approach [e.g. *Anderson*, 1995]. This implies assuming a-priori existing weak layer fractures having zero or negligible strength (so-called deficit zones). In this paper, we call these fractures "sub-critical weak layer fractures" to emphasize that they are smaller than the size necessary to result in fast fracture propagation. Currently no data exist on what happens to sub-critical weak layer fractures over time in terms of whether they sinter, and how fast that sintering process might occur. The work of *de Montmollin* [1982] suggests that fast sintering times might be possible, and new measurements indicate even sub-second sintering might occur [*Schneebeli and Szabo*, preprint, 2005]. In a recent model, *Fyffe and Zaiser* [2004] point out that no published *in-situ* observations of sintering speed currently exist, so they estimate the typical time for a layer to re-sinter to its original strength to be 10 s with a range of 1 to 10^5 s.

In addition to the sub-critical fractures discussed above, sometimes the weak layer under entire slopes or parts of slopes fractures as a slope collapses with a distinct "whumpf" sound [*Johnson, et al.*, 2004]. This often triggers an avalanche in steeper terrain, occasionally from great distances. However, other times no avalanches are triggered, and the extent of the fracture is only observable due to visible tensile cracks on the snow surface. The absence of avalanches in these situations may be due to the peripheral strength of the slab, the terrain (e.g., insufficient slope angle for avalanche initiation), or some other unknown cause. Reports of slabs releasing some time after the fracture are rare, and many avalanche professionals consider these slopes to be more stable than prior to the fracture. Yet we know of no rigorous measurements of point stability on slopes that have collapsed, and no published guidance exists for avalanche workers on how to approach collapsed slopes in terms of their post-collapse stability.

This paper provides new insights into weak layer changes after fracturing by investigating temporal changes in shear strength and point snow stability for two fractured weak layers. In both cases, weak layer strength decreased immediately after fracturing followed by pronounced strengthening through time. These results have implications for both modeling snow slab release and for operational stability assessment.

2. Data and Methods

In the course of studies on spatial variability of snowpack properties in Switzerland [*Kronholm,* 2004] and southwestern Montana (U.S.A.) [*Logan,* 2005], we unintentionally fractured slopes while testing the slab and weak layer. In two cases the targeted weak layer collapsed with an audible “whumpf” and visible tensile cracks but no avalanche released, offering unique opportunities to collect data with measurements before and after the fracture. Our data cover an area the size of a small slope, so some trends may be due to the changes in spatial location of the data points. The spatial trends are neglected here. We described snow layer characteristics according to *Colbeck et al.* [1990].

Our first dataset comes from a north-facing slope near Davos, Switzerland (Eastern Swiss Alps, 46° 49' N, 9° 50' E) sampled on 1 March 2002. The snowpack consisted of a 50 cm thick slab layer of small (0.25 - 0.75 mm) primarily rounded and partly faceted crystals overlying a weak layer of larger rounded facets and depth hoar crystals (1.5 - 2.5 mm) sitting on top of a melt-freeze crust. Slope angles vary from 34° in the upper part of the sampled area to 25° at the bottom. We conducted 24 stability measurements using the rammrutsch test [*Schweizer et al.*, 1995] in an 18 m × 18 m area of the slope (Figure 1). The rammrutsch test progressively loads an isolated 30 cm × 30 cm column of snow by dropping a 1 kg weight from increasing heights onto a plate placed on the column. Stability is measured as the drop height necessary to fracture the weak layer within the column. Of 24 tests, 10 did not fracture in the specific weak layer, either because the maximum drop height of 1 m was reached or because a fracture occurred in a lower weak layer. Therefore we had 14 test results for our analyses. Comparing the two datasets required converting the Swiss stability data into approximate shear strength [*Jamieson*, 1995, 1999; *Stewart*, 2002] in order to calculate a strengthening rate. We used the collapse time, the time of the last sampling, and the typical test time to convert the test sequence into approximate time.

Our second dataset comes from a northeast facing slope near West Yellowstone, Montana, U.S.A. (44° 45’ N, 111° 15’ W). The slope is inclined relatively uniformly at about 28°. Sampled on 7 February 2004, the 170 cm deep snowpack fractured on a layer of surface hoar buried 55 cm below the surface. The weak layer structure consisted of two individual layers of surface hoar stacked on top of each other. After the slope collapsed, we observed that the upper of the two layers collapsed, with the lower surface hoar layer largely intact. A variety of snow crystal types comprised the slab, with a thin melt-freeze crust immediately above the surface hoar layer.

We utilized a 250 cm^2 shear frame to measure the shear strength of the buried surface hoar layer for the Montana dataset [*Jamieson and Johnston,* 2001]. The shear frame test involves placing a shear frame to within a few mm above the targeted weak layer, then pulling the frame with a force gauge until the weak layer fractures. The slope was sampled in a 31 m × 31 m cross-shaped area (Figure 2). The tests consistently fractured planar and smooth at the targeted weak layer, and the dataset includes 14 tests conducted prior to, and 34 tests after, the slope collapsed. Again, we approximated test times from test sequence using several recorded test times for guidance. In addition, we collected data on the day following the collapse.

While calculating the weak layer strengthening rate by analyzing the post-fracture data using a least-squares linear regression, two outliers were removed due to their inordinate leverage on the regression equation as measured by Cook's distance [*Statsoft*, 1999]. Excessively high values of shear strength at those two points may be due to improper shear frame placement, or some other unknown cause. We compared samples of shear strength values from collapsed and uncollapsed areas using the non-parametric Mann-Whitney U-test. Observed differences were judged to be statistically significant where the level of significance is $p < 0.05$.

3. Results

For the Swiss dataset, we report the stability before and after the collapse expressed as rammrutsch drop height and calculated shear strength (Figure 3). Before the slope collapsed one rammrutsch test (number 4) fractured in the specific weak layer, while three tests (1, 2 and 3) did not. Tests 7 and 8 also did not fracture in the weak layer. This, together with the relatively high drop heights for tests 9 and 10, leads us to believe that the fracture did not propagate to the lowest row of tests, possibly due to the more gentle inclination of that part of the slope. Immediately following the collapse, drop heights decreased to low values (10 cm) before subsequently strengthening at an apparently increasing rate. It took about 1.5 hours to reach pre-collapse strength, and drop height results of   30 cm after about 2 hours indicated considerable weak layer strengthening. Converting drop height to shear strength resulted in an increase of about 300 Pa h^{-1}. Though limited, the Swiss data demonstrate that rapid strengthening can occur in a weak layer within hours after a collapse. The strength increase is probably due to sintering as the grains re-locate and pack after the collapse.

At our Montana site, shear strength decreased markedly after the slope collapsed, creating distinct groups of pre- and post-collapse measurements (Figure 4). From the pre-collapse value of about 1100 Pa, shear strength immediately after the collapse significantly decreased to about 300 Pa ($p < 0.0001$). The median stability index, which is simply the shear strength divided by the shear stress applied by the weight of the overlying slab, dropped from over 3 to about 1.2. Interestingly, seven of the first ten shear frame tests following the fracture had stability ratios less than 1.

Post-collapse strengthening of the Montana weak layer also occurred, but at a slower rate than the Swiss dataset. Regression analysis revealed an approximately linear strengthening rate of about 70 Pa h^{-1} (Figure 4). At this rate it would take about 10 hours for the layer to recover its original strength. On the day following the collapse, we sampled another area of the slope. At that time and location, the shear strength in the collapsed area did not significantly differ from that in the uncollapsed area ($p = 0.88$), indicating the layer strengthened to the pre-collapse value. That part of the slope exhibited lower median shear strength than the part of the slope sampled the previous day, possibly due to spatial variation in weak layer strength.

4. Discussion and Conclusions

Both datasets show significant decreases in weak layer shear strength following fracturing, though some residual strength remains. After the collapse, weak layers strengthened at rates at least 15 times faster than the 100 Pa d^{-1} rate characteristic of unfractured weak layers [*Jamieson and Johnston*, 1999]. Typically, uncollapsed weak layers gain strength through a combination of increasing numbers of bonds, and an increase in the strength of existing bonds [*Jamieson and Schweizer*, 2000]. On the other hand, with fractured weak layers the old bonds will be broken, but the number of potential new bonds will increase dramatically, resulting in rapid sintering. The difference in strengthening rates between our two sites is likely due to the differences between the two weak layers. The first weak layer consisted of depth hoar and rounded facets, with numerous points of contact for sintering. The second layer consisted of two surface hoar layers stacked on top of each other, and the collapse occurred within the upper layer. This arrangement likely resulted in fewer post-collapse contact points for sintering, and the large crystal size may have also contributed to the slower sintering rate at this site [*Colbeck*, 2001]. Many complicating factors likely affect sintering rates, including the current load on the weak layer, whether further load (i.e., new or windblown snow) is being added to the snowpack, and the characteristics of the layers surrounding the weak layer. Clearly, many more of these unique datasets are needed to definitively establish sintering rate guidelines for fractured weak layers.

Our results have implications for better understanding and modeling dry snow slab avalanche release. These limited data show that large weak layer fractures will retain some residual strength and will sinter relatively quickly. This implies that the sub-critical weak layer fractures (i.e., weak layer fractures that are smaller than the critical size necessary to trigger an avalanche) that are postulated to be a pre-requisite for slab avalanche release in many models [e.g., *Bader and Salm*, 1990] are relatively transient phenomena. Without continued loading or sizable additional creep forces, such zones are likely to heal to the pre-fracture or greater strength within hours or perhaps up to a day after the fracture. Given our results, realistic numerical snow slab release models should include a fracture initiation process based on both fracturing and sintering of bonds in addition to fracture propagation (such as has been done recently by *Fyffe and Zaiser* [2004]), rather than simply assuming a-priori existing sub-critical weak layer fractures.

From a practical perspective, both datasets indicate significant decreases in weak layer strength after fracturing, implying that slope stability might also decrease. However, though avalanche professionals generally treat collapsed slopes with care, many of them believe slope stability increases immediately following a collapse. Clearly many other factors besides shear strength, such as the energy necessary to drive fracture propagation or stress relaxation, affect slope stability. Our work reinforces the idea that stability tests must be interpreted carefully, and their interpretation must be supplemented with varied additional information for effective avalanche forecasting [*McClung*, 2002]. Further, until we better understand all the dominant factors involved in slope stability, avalanche workers should continue to use caution around collapsed slopes.

Acknowledgements. We greatly appreciate the field help of E. Lutz in Montana, and J. Hendrikx and A. Heilig in Switzerland. B. Jamieson, I. McCammon, E. Lutz, and E. Greene provided many useful comments on this subject. R. Elliot, L. Fitzgerald, and T. Leonard shared their vast practical experience with collapsed slopes. Two anonymous reviewers provided useful and constructive criticisms. The U.S. National Science Foundation (Grant #BCS-024310, K. Hansen, P.I.) and Swiss National Science Foundation (Project No. 2000-066643.01) provided partial support for this work.

References

Anderson, T. L. (1995), *Fracture Mechanics: Fundamentals and Applications, 2nd edition,* 688 pp., CRC Press, Boca Raton, U.S.A.

Bader, H., and B. Salm (1990), On the mechanics of snow slab release, *Cold Reg. Sci. Technol.*, *17*, 287-299.

Colbeck, S. C. (1991), The layered character of snow covers, *Rev. Geophys.*, *29*, 81-96.

Colbeck, S.C. (2001), Sintering of unequal grains, *J. Appl. Phys., 89(8),* 4612-4618.

Colbeck, S. C., E. Akitaya, R. Armstrong, H. Gubler, J. Lafeuille, K. Lied, D. McClung, and E. Morris (1990), *The international classification of seasonal snow on the ground*, 23 pp., International Commission on Snow and Ice, Int. Assoc. Hydrol. Sci., Wallingford, Oxfordshire, U.K.

de Montmollin, V. (1982), Shear tests on snow explained by fast metamorphism, *J. Glaciol., 28*, 187-198.

Fyffe, B., and M. Zaiser (2004), The effects of snow variability on slab avalanche release, *Cold Reg. Sci. Technol.*, *40*, 229-242.

Jamieson, J. B. (1995), Avalanche prediction for persistent snow slabs, Ph.D. thesis, 258 pp., University of Calgary, Calgary AB, Canada.

Jamieson, J. B. (1999), The compression test - after 25 years, *The Avalanche Review*, *18*, 10-12.

Jamieson, J. B., and C. D. Johnston (1999), Snowpack factors associated with strength changes of buried surface hoar layers, *Cold Reg. Sci. Technol.*, *30*, 19-34.

Jamieson, J. B., and J. Schweizer (2000), Texture and strength changes of buried surface hoar layers with implications for dry snow-slab avalanche release, *J. Glaciol., 46*, 151-160.

Jamieson, J. B., and C. D. Johnston (2001), Evaluation of the shear frame test for weak snowpack layers, *Ann. Glaciol.*, *32*, 59-68.

Johnson, B. C., J. B. Jamieson, and R. R. Stewart (2004), Seismic measurement of fracture speed in a weak snowpack layer, *Cold Reg. Sci. Technol.*, *40*, 41-45.

Kronholm, K. (2004), Spatial variability of snow mechanical properties with regard to avalanche formation, Ph. D. thesis, 187 pp, University of Zurich, Zurich.

Logan, S. (2005), Temporal changes in the spatial patterns of weak layer shear strength and stability on uniform slopes, M. Sc. thesis, 157 pp., Montana State University, Bozeman, Montana.

Louchet, F. (2001), A transition in dry-snow slab avalanche triggering modes, *Ann. Glaciol.*, *32*, 285-289.

McClung, D. M. (1979), Shear fracture precipitated by strain softening as a mechanism of dry slab avalanche release, *J. Geophys. Res.*, *84*, 3519-3526.

McClung, D. M. (1981), Fracture mechanical models of dry slab avalanche release, *J. Geophys. Res.*, *86*, 10783-10790.

McClung, D. M. (2002), The elements of applied forecasting - Part II: The physical issues and the rules of applied avalanche forecasting, *Natural Hazards*, *26*, 131-146.

Schweizer, J. (1999), Review of dry snow slab avalanche release, *Cold Reg. Sci. Technol.*, *30*, 43-57.

Schweizer, J., J. B. Jamieson, and M. Schneebeli (2003), Snow avalanche formation, *Rev. Geophys.*, *41*, 1016, doi:10.1029/2002RG000123.
Schweizer, J., M. Schneebeli, C. Fierz, and P. M. B. Föhn (1995), Snow mechanics and avalanche formation: Field experiments on the dynamic response of the snow cover, *Surv. Geophys.*, *16*, 621-633.
Statsoft (1999), *Statistica*, Tulsa, Oklahoma.
Stewart, W. K. (2002), Spatial variability of slab stability within avalanche start zones, M. Sc. Thesis, 103 pp., University of Calgary, Calgary, Alberta.
Stoffel, M., and P. Bartelt (2003), Modelling snow slab release using a temperature-dependent viscoelastic finite element model with weak layers, *Surv. Geophys., 24(5-6),* 417-430.

Figures

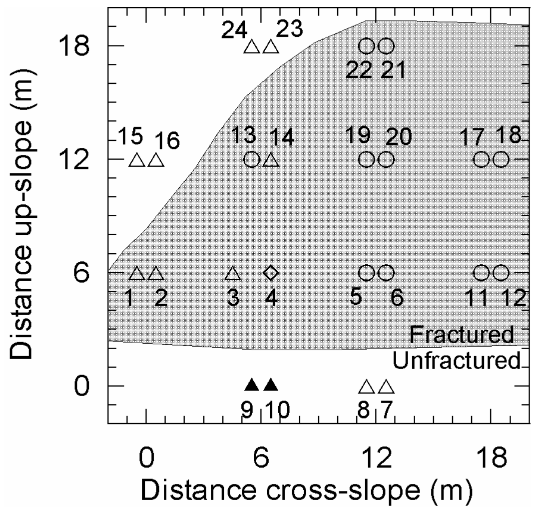

Figure 1: Rammrutsch sampling locations at the Swiss site, with the numbers indicating the test order. Gray area indicates the assumed extent of the fracture within the study area. Open triangles represent points not used in the analysis because they did not fracture on the targeted weak layer. Filled triangles represent points where the fracture occurred in the targeted weak layer, but are located outside our assumed weak layer collapse area. The diamond represents the test prior to the collapse, and the circles are post-collapse data points.

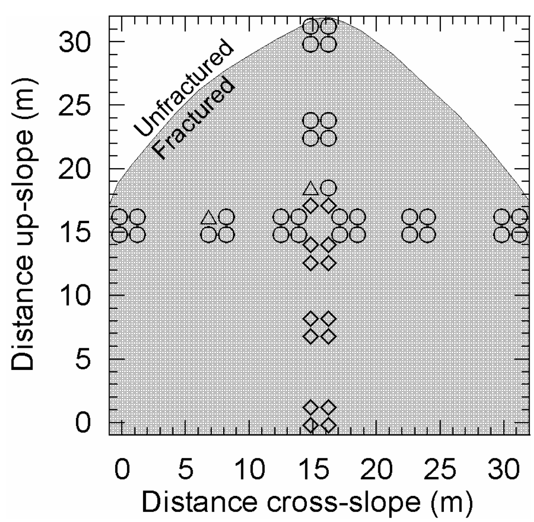

Figure 2: Shear frame test locations at our Montana site. Gray area indicates the assumed extent of the fracture within the study area. Diamonds indicate samples taken before the collapse, circles show the post-collapse measurements, and the two triangles represent outliers not considered in the calculation of the sintering rate (see Figure 4).

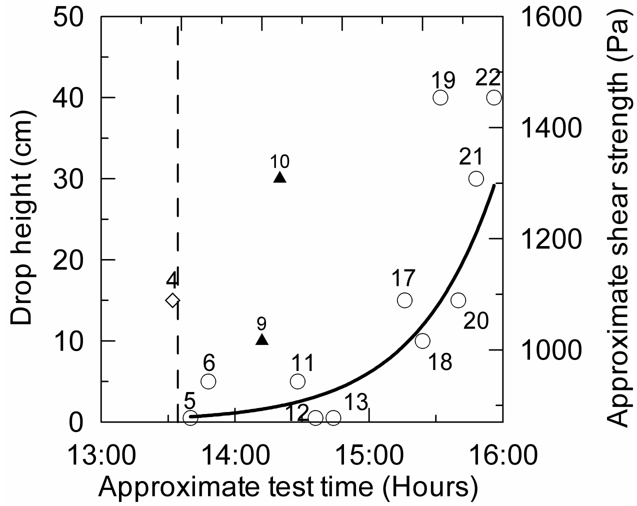

Figure 3: Rammrutsch drop height plotted versus approximate test time shows an increasing strengthening rate of the weak layer. The collapse occurred at the vertical dashed line. Same symbols as in Figure 1.

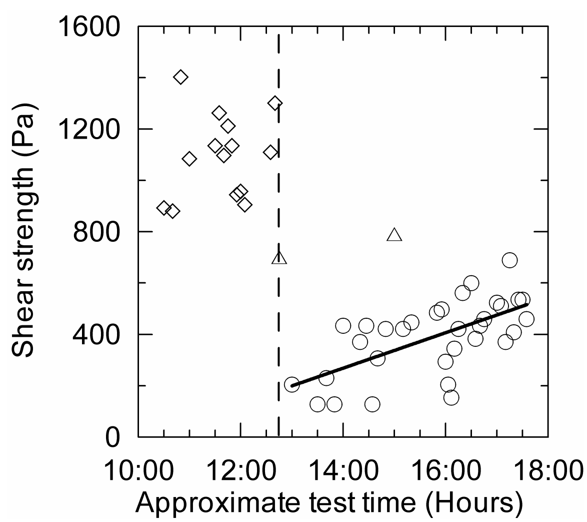

Figure 4: Plotting shear strength versus the approximate time of the test at the Montana site shows: 1) a significant decrease following the collapse (indicated by the dashed line), and 2) a roughly linear increase in shear strength through time following the collapse, with a rate of about 70 Pa h^{-1}. The triangles represent outliers removed from the analysis before calculating the strengthening rate.